UNC-89 (obscurin) binds to MEL-26, a BTB-domain protein, and affects the function of MEI-1 (katanin) in striated muscle of *Caenorhabditis elegans*

Kristy J. Wilson[a], Hiroshi Qadota[a], Paul E. Mains[b], and Guy M. Benian[a]
[a]Department of Pathology, Emory University, Atlanta, GA 30322; [b]Department of Biochemistry and Molecular Biology, University of Calgary, Calgary, AB T2N 1N4, Canada

ABSTRACT **The ubiquitin proteasome system is involved in degradation of old or damaged sarcomeric proteins. Most E3 ubiquitin ligases are associated with cullins, which function as scaffolds for assembly of the protein degradation machinery. Cullin 3 uses an adaptor to link to substrates; in *Caenorhabditis elegans*, one of these adaptors is the BTB-domain protein MEL-26 (maternal effect lethal). Here we show that MEL-26 interacts with the giant sarcomeric protein UNC-89 (obscurin). MEL-26 and UNC-89 partially colocalize at sarcomeric M-lines. Loss of function or gain of function of *mel-26* results in disorganization of myosin thick filaments similar to that found in *unc-89* mutants. It had been reported that in early *C. elegans* embryos, a target of the CUL-3/MEL-26 ubiquitylation complex is the microtubule-severing enzyme katanin (MEI-1). Loss of function or gain of function of *mei-1* also results in disorganization of thick filaments similar to *unc-89* mutants. Genetic data indicate that at least some of the *mel-26* loss-of-function phenotype in muscle can be attributed to increased microtubule-severing activity of MEI-1. The level of MEI-1 protein is reduced in an *unc-89* mutant, suggesting that the normal role of UNC-89 is to inhibit the CUL-3/MEL-26 complex toward MEI-1.**

Monitoring Editor
William P. Tansey
Vanderbilt University

Received: Jan 24, 2012
Revised: May 9, 2012
Accepted: May 17, 2012

INTRODUCTION

In muscle, the overall mass and number of sarcomeres are maintained by a fine balance between removal and degradation of old or damaged proteins and replacement by newly synthesized proteins. During muscle atrophy in humans, this balance is disrupted, with a net loss of sarcomeres and muscle mass. Muscle atrophy is attributable to muscle disuse (immobilization, microgravity of space travel) or starvation and occurs in many chronic diseases (renal failure, diabetes, cancer cachexia, sepsis, and burn injury) and also in elderly patients without underlying disease (in which case it is termed sarcopenia; Murton and Greenhaff, 2009). During muscle atrophy, both the degradation of myofibrillar proteins is up-regulated and the synthesis of myofibrillar proteins is down-regulated.

The major system mediating protein degradation in muscle is the ubiquitin proteasome system (Ventadour and Attaix, 2006; Murton *et al.*, 2008). The 76-residue ubiquitin is covalently attached to a substrate, and this directs it to the proteasome for degradation. Ubiquitination involves multiple enzymes, including a ubiquitin-activating enzyme (E1), a ubiquitin-conjugating enzyme (E2), and a ubiquitin protein ligase (E3). The majority of E3s are associated with cullin "really interesting new gene" (RING) ligases (CRLs), in which a cullin acts as a scaffold for assembly of an E3 (contains a RING Zn finger domain), a protein that recognizes a substrate (a substrate recognition subunit [SRS], usually containing an F box domain [first identified in cyclin F]), and, with the exception of Cul3-type CRLs, an adaptor subunit that links the SRS to the complex (Petroski and Deshaies, 2005; Bosu and Kipreos, 2008). There are five types of cullins: Cul1–5. For Cul3 CRLs the functions of the F box protein and the adaptor subunit are served by a single protein that contains a BTB domain (a dimerization domain; named for BR-C, ttk, and bab—the first three proteins found to have this domain). The BTB domain

This article was published online ahead of print in MBoC in Press (http://www.molbiolcell.org/cgi/doi/10.1091/mbc.E12-01-0055) on May 23, 2012.

Address correspondence to: Guy Benian (pathgb@emory.edu).

Abbreviations used: CRL, cullin RING ligase; ECL, enhanced chemiluminescence; GFP, green fluorescent protein; GST, glutathione *S*-transferase; HA, hemagglutinin; HRP, horseradish peroxidase; IK, interkinase region; MATH, meprin and TRAF homology; MBP, maltose-binding protein; MEL-26, maternal effect lethal; NGM, nematode growth media; RING, "really interesting new gene"; RNAi, RNA interference; SAGE, Serial Analysis of Gene Expression; SRS, substrate recognition subunit.

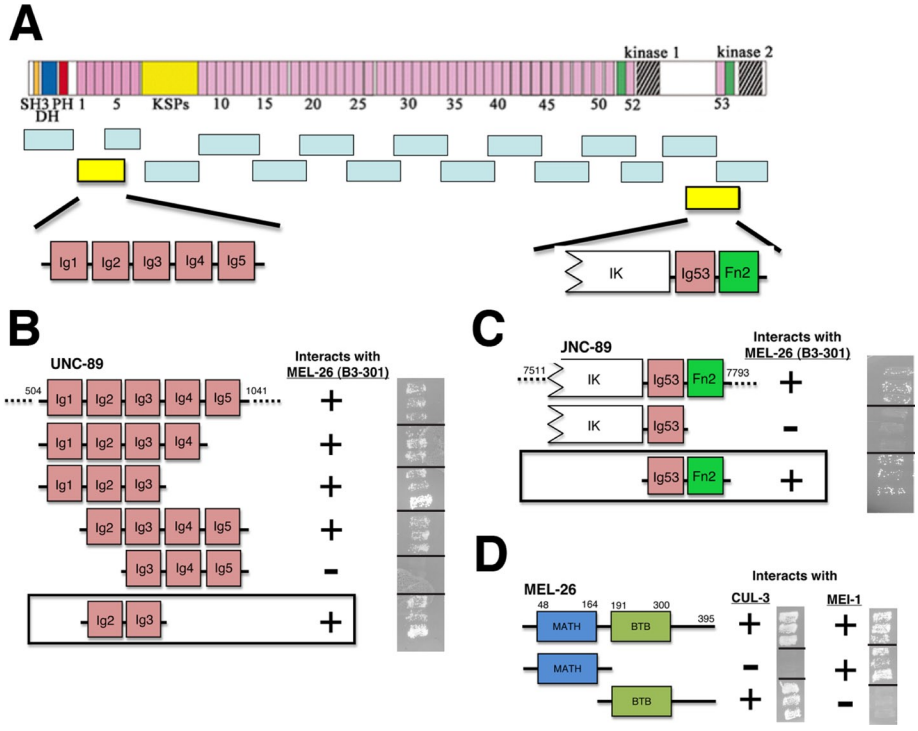

FIGURE 1: MEL-26 interacts with two regions of UNC-89. (A) A yeast two-hybrid library screen using UNC-89 Ig1–5 recovered one prey representing MEL-26. When MEL-26 was used to screen the other 16 segments that comprise UNC-89-B, interaction was also found with 1/3IK-Ig53-Fn2. (B) With the use of deletion derivatives of Ig1–5, yeast two-hybrid assays revealed that the minimal region required for interaction with MEL-26 is Ig2–Ig3. (C) With the use of deletion derivatives of 1/3IK-Ig53-Fn2, yeast two-hybrid assays revealed that the minimal region required for interaction with MEL-26 is Ig53–Fn2. (D) Two-hybrid assays with the indicated portions of MEL-26 showed that the BTB domain of MEL-26 is sufficient for interaction with CUL-3, and that the MATH domain of MEL-26 is sufficient for interaction with MEI-1. In B–D, to the right of each row are images of yeast growth of three independent colonies on plates lacking adenine (–Ade) for B and D and on plates lacking histidine (–His) for C.

binds directly to Cul3, and other domains in the protein (e.g., a protein–protein interaction meprin and TRAF homology [MATH] domain) bind to specific substrates. During muscle atrophy of rodents and humans, two components of muscle-specific E3s are up-regulated—muscle ring finger protein-1 (RING finger E3) and atrogin-1 (F box protein) (Bodine *et al.*, 2001; Gomes *et al.*, 2001). Mice knocked out for either protein are partially resistant to muscle atrophy.

The nematode *Caenorhabditis elegans* is a proven platform for discovery of new information about conserved sarcomere components and for discovery of new and conserved sarcomere components (Waterston, 1988; Moerman and Fire, 1997; Moerman and Williams, 2006; Qadota and Benian, 2010; Benian and Epstein, 2011). The *C. elegans* gene *unc-89* (uncoordinated) encodes a set of giant polypeptides of up to 900,000 Da that are located at the sarcomeric M-line (Benian *et al.*, 1996; Small *et al.*, 2004; Ferrara *et al.*, 2005). The human homologue of UNC-89 is called obscurin (Bang *et al.*, 2001; Young *et al.*, 2001; Fukuzawa *et al.*, 2005; Kontrogianni-Konstantopoulos *et al.*, 2009). Loss of function of *unc-89* results in adult worms with disorganization of the myofilament lattice, usually a lack of M-lines, and with decreased locomotion (Waterston *et al.*, 1980; Benian *et al.*, 1999). The largest UNC-89 isoform consists of 53 Ig domains, two Fn3 domains, two protein kinase domains at its C-terminus, and SH3, DH, and PH domains at its N-terminus. The DH domain of UNC-89 has exchange activity for RHO-1 (the RhoA orthologue in *C. elegans*). Partial knockdown of *rho-1* in adult worms results in a pattern of disorganization of myosin thick filaments similar to loss of function of *unc-89* (Qadota *et al.*, 2008a).

The large size of UNC-89 precludes many biochemical methods for analyzing its role in sarcomere assembly and maintenance. Thus we are systematically identifying the binding partners of UNC-89, beginning with yeast two-hybrid screens, and then determining the intracellular localization and mutant phenotypes of putative interactors. We previously reported that the protein kinase domain–containing region of UNC-89 interacts with SCPL-1, a CTD-type protein phosphatase, and with LIM-9, a homologue of human FHL (Qadota *et al.*, 2008b; Xiong *et al.*, 2009). Here we report that two portions of UNC-89 interact with MEL-26 (maternal effect lethal), a BTB-domain protein previously shown to interact with CUL-3 (cullin 3) and to be essential in early embryonic development (Dow and Mains, 1998; Furukawa *et al.*, 2003; Pintard *et al.*, 2003; Xu *et al.*, 2003). By immunolocalization, we find that MEL-26 colocalizes with UNC-89 at M-lines. Of importance, we demonstrate that mutations in *mel-26* and *cul-3* result in disorganization of sarcomeric thick filaments similar to mutations in *unc-89*. MEI-1 (meiosis defective), the catalytic subunit of the nematode orthologue of the microtubule-severing complex katanin, is a known substrate for ubiquitylation by the CUL-3/MEL-26 complex in early embryos. We show that mutation in *mei-1* also disrupts thick filament organization similar to *unc-89* and *mel-26*. We provide genetic evidence that at least some of the *mel-26* loss-of-function phenotype can be attributed to increased microtubule-severing activity of MEI-1. We demonstrate that the level of MEI-1 protein is reduced in an *unc-89* mutant, indicating that the normal role of UNC-89 is to inhibit the CUL-3/MEL-26 complex toward MEI-1 in striated muscle. Our results suggest a novel mechanism for regulating protein degradation in muscle, and this has a role in thick-filament assembly and/or maintenance.

RESULTS

UNC-89 is a binding partner of MEL-26, a substrate adaptor for CUL-3

As part of our systematic search for binding partners for the giant modular protein UNC-89, we used a five-domain segment of UNC-89, Ig1–Ig5, as bait to screen a library of *C. elegans* cDNA using the yeast two-hybrid system (Xiong, Qadota, and Benian, unpublished data). One of the preys was found to encode MEL-26. We wanted to determine whether MEL-26 interacted with any other regions of UNC-89. Thus we examined a "bookshelf" containing 16 overlapping yeast two-hybrid bait plasmids covering the whole coding sequence of UNC-89. In addition to Ig1–Ig5, MEL-26 also interacted with a region between the two kinase domains of UNC-89, including approximately one third of the interkinase region (IK), Ig53, and Fn2 domains (Figure 1A). Using yeast-two hybrid assays, we identified the minimal portions of each UNC-89 fragment that are necessary and

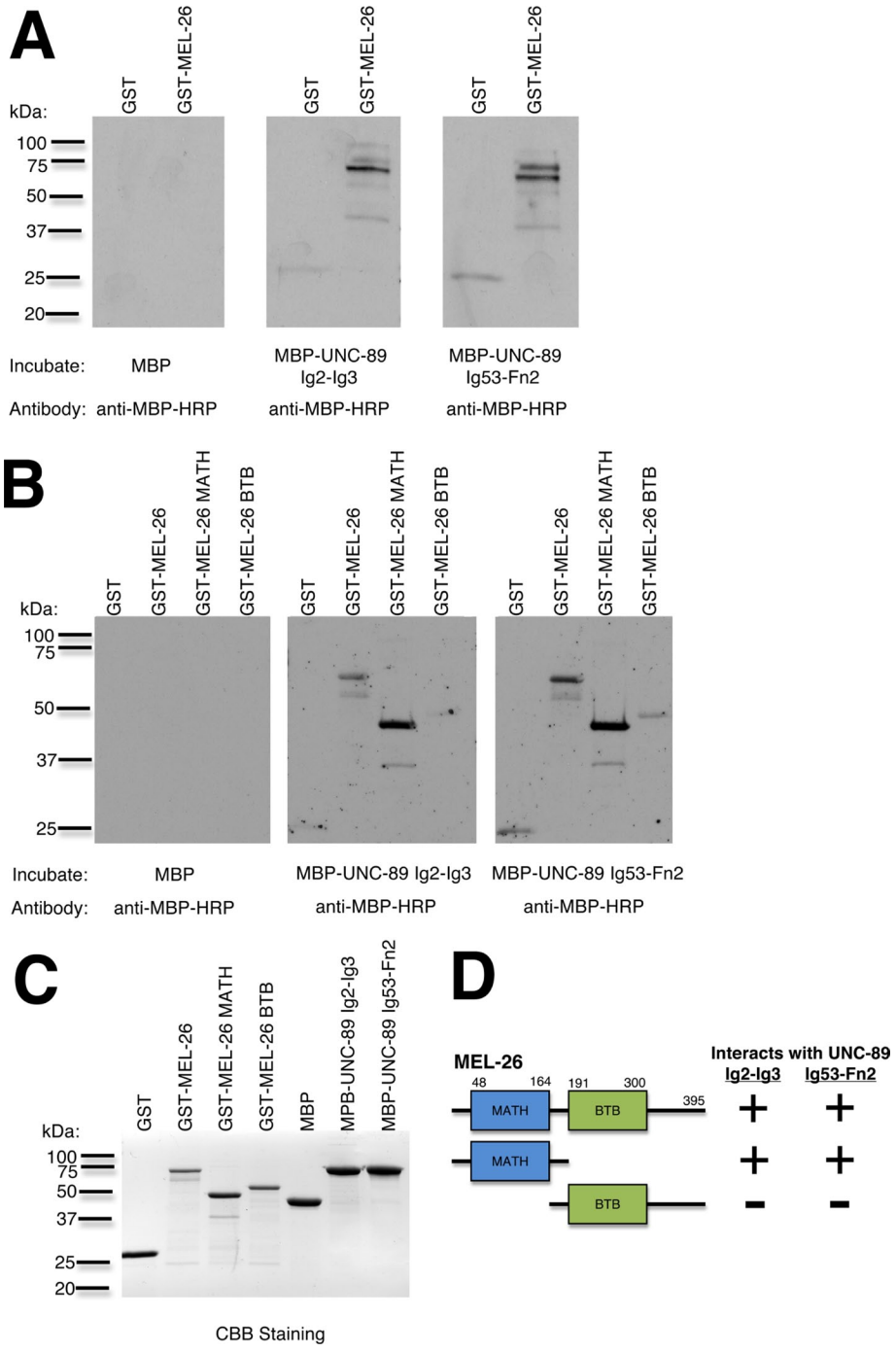

FIGURE 2: Far Western assays with purified proteins verify the UNC-89/MEL-26 interactions and show that only the MATH domain of MEL-26 is required. (A) Pairs of GST and full-length GST-MEL-26 were separated by SDS–PAGE, transferred to a membrane, reacted with MBP, MBP-UNC-89 Ig2–Ig3, or MBP-UNC-89 Ig53–Fn2, washed, incubated with anti–MBP-HRP, washed, and detected by ECL. As shown, GST-MEL-26, but not GST, reacted with both UNC-89 fragments. (B) Three sets of GST, GST-MEL-26, GST-MEL-26 MATH, and GST-MEL-26 BTB were separated by SDS–PAGE and transferred to membranes, and the indicated reactions were performed. Note that GST-MEL-26 and GST-MEL-26-MATH, but not GST or GST-MEL-26 BTB, showed interaction with both fragments of UNC-89. (C) SDS PAGE stained with Coomassie brilliant blue (CBB) of all the proteins (2 μg each) used in the far Western assays shown in A and B. (D) Schematic summary of the far Western results.

sufficient to interact with MEL-26. As shown in Figure 1, B and C, Ig2–Ig3 and Ig53–Fn2, are minimally required to interact with MEL-26. It is worth noting that MEL-26 interacts with a different minimal region of UNC-89 than does CPNA-1, the other protein identified in the original screen (Xiong *et al.*, unpublished data), which interacts minimally with UNC-89 Ig1–Ig2–Ig3. Despite the multitude of other Ig domains present in UNC-89, MEL-26 only interacts with UNC-89 Ig2–Ig3 and Ig53–Fn2, indicating specificity.

MEL-26 is part of a CRL complex and acts as an adaptor to bring together the substrate and CUL-3 (Cul3) for ubiquitination (Furukawa *et al.*, 2003; Pintard *et al.*, 2003; Xu *et al.*, 2003). MEL-26 contains an N-terminal MATH domain and a C-terminal BTB domain. It has been reported that the BTB domain of MEL-26 interacts with CUL-3, and that the MATH domain of MEL-26 interacts with a substrate, MEI-1 (Luke-Glaser *et al.*, 2007b). Using two-hybrid assays, we verified that the MATH domain interacts with MEI-1 and that the BTB domain interacts with CUL-3 (Figure 1D). In addition, we confirmed the yeast two-hybrid interactions between UNC-89 and MEL-26 using far Western assays with purified proteins (Machida and Mayer, 2009). UNC-89 Ig2–Ig3 and UNC-89 Ig53–Fn2 each interacts with MEL-26 (Figure 2A). We also found that both UNC-89 fragments interact with the MATH domain but not the BTB domain of MEL-26 (Figure 2B). Thus, portions of UNC-89 interact with the same domain of MEL-26 as MEI-1 (Figure 2D).

We next reasoned that if UNC-89 and MEL-26 interact in vivo, MEL-26 should colocalize with UNC-89 in the sarcomere. Antibodies to MEL-26 (kindly provided by Lionel Pintard, University of Paris, Paris, France) were used to immunostain whole fixed adult nematodes together with marker antibodies for sarcomeric M-lines (UNC-89) and dense bodies (α-actinin). As shown in Figure 3, anti–MEL-26 localizes in a striated pattern to both M-lines and I-bands (and probably dense bodies). Colocalization of MEL-26 with UNC-89 at M-lines is consistent with MEL-26 and UNC-89 interacting in vivo. Of interest, sarcomeric localization of MEL-26 in adult muscle is in contrast to the diffuse localization of MEL-26 reported in early-stage embryos (Luke-Glaser *et al.*, 2007a). To our knowledge, this is the first time that a component of a cullin complex has been localized in the sarcomere.

unc-89 and *mel-26* mutants have similar defects in thick-filament assembly and/or maintenance

Loss of function for *unc-89* results in adult worms having disorganized sarcomeres, especially in the A-band, and usually they have no M-lines (Waterston *et al.*, 1980; Benian *et al.*, 1999). We showed

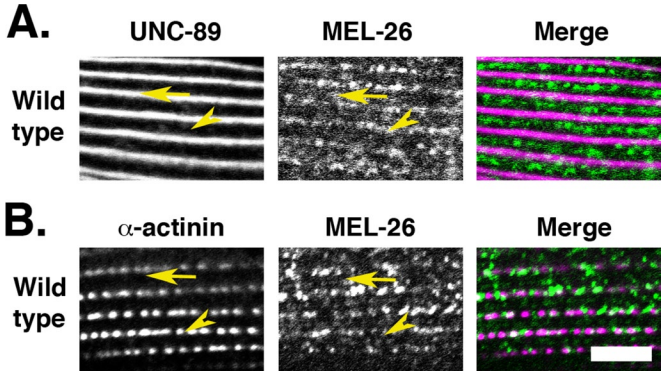

FIGURE 3: MEL-26 localizes to M-lines and I-bands in adult body-wall muscle. Wild type *C. elegans* adults were immunostained with either anti–UNC-89 (M-lines) and anti–MEL-26 (A) or anti–α-actinin (dense bodies) and anti-MEL-26 (B) and imaged by confocal microscopy. Arrows mark the position of M-lines as detected by anti-UNC-89, and arrowheads mark the position of dense bodies as detected by anti–α-actinin. In the merged images, white indicates colocalization of signals. Bar, 5 μm.

previously that one of the most severe alleles of *unc-89*, *su75*, lacks expression of all the giant isoforms of UNC-89 (Small *et al.*, 2004), including one region, Ig2–Ig3, that we showed interacts with MEL-26. In addition, *unc-89(su75)*, when immunostained with antibodies to myosin A (MHC A) or visualized with green fluorescent protein (GFP)::MHC A, displays disorganization of thick filaments, including what appear to be abnormal aggregates of myosin, and V-shaped crossing of A-bands (Qadota *et al.*, 2008a). Thus, we wondered whether loss of function of either *mel-26* or *cul-3* might show a similar disorganization of thick filaments. We used RNA interference (RNAi) to knock down either *mel-26* or *cul-3*, beginning at the L1 larval stage, to avoid embryonic lethality in a strain expressing GFP::MHC A. As shown in Figure 4A, knockdown of either *mel-26* or *cul-3* resulted in adults having body-wall muscle with disorganized thick filaments, in a pattern similar to that of *unc-89(su75)*. In fact, *cul-3(RNAi)* consistently resulted in thick-filament disorganization more severe than that found in *unc-89(su75)* or *mel-26(RNAi)*. These results suggest that in striated muscle, CUL-3 may act through MEL-26 and additional BTB-containing adaptor proteins. Alternatively, RNAi might be more effective for *cul-3* than it is for *mel-26*.

To confirm the RNAi results for *mel-26*, we investigated the adult muscle phenotype of an allele of *mel-26*, *ct61sb4*. Although null, this allele is temperature sensitive (Lu and Mains, 2007), and so embryonic lethality can be bypassed at 15°C. We stained these *mel-26* mutant adult worms with anti-MHC A. As shown in Figure 4B, *mel-26(ct61sb4) unc-29(e1072)*, but not *unc-29(e1072)* (a linked marker used for strain construction; see *Materials and* Methods), shows disorganization of thick filaments similar to that observed by RNAi for *mel-26*.

For most genes, loss of function and gain of function will yield different phenotypes. Thus we wondered how the gain of function of *mel-26* might compare to the loss of function of *mel-26*. To examine this, we expressed hemagglutinin (HA)-tagged MEL-26 from a heat shock promoter in adult worms. As shown in Figure 4C, HA-MEL-26 is expressed in nematodes only after heat shock. Unexpectedly, in muscle cells that overexpress MEL-26 (Figure 4D), thick filaments are disorganized in a way that is very similar to loss of function of *mel-26* by RNAi or by mutation. Heat shock itself had no effect on the organization of thick filaments (Figure 4E).

mel-26 muscle defects are mediated by *mei-1* microtubule-severing activity

MEI-1 is the *C. elegans* orthologue of the microtubule-severing enzyme katanin (Srayko *et al.*, 2000; Roll-Mecak and McNally, 2010) and has been identified as a target of the MEL-26/CUL-3 ubiquitylation complex in *C. elegans* embryos (Furukawa *et al.*, 2003; Pintard *et al.*, 2003; Xu *et al.*, 2003). MEI-1 has a well-established function in meiotic spindle formation of newly fertilized *C. elegans* embryos (Srayko *et al.*, 2000, 2006; McNally *et al.*, 2006; McNally and McNally, 2011). Low levels of *mei-1* mRNA have been reported at other stages (Clark-Maguire and Mains, 1994a). We sought evidence that MEI-1 is expressed in adult somatic cells, which include muscle. For this, we used a temperature-sensitive mutant in *glp-4* (germline proliferation defective). *glp-4(bn2ts)* mutants raised at the restrictive temperature of 25°C have only a few germ cell precursors, all arrested at the prophase of the mitotic cell cycle, with none entering meiosis (Beanan and Strome, 1992). As shown in Figure 5A, by immunoblot MEI-1 can be detected from these adults that lack a germline. Consistent with this somatic expression, Serial Analysis of Gene Expression (SAGE data), available at WormBase (www.wormbase.org), indicate that in wild-type nematodes, *mei-1* mRNA is expressed in multiple somatic cell types, including body-wall muscle cells, hypodermal cells, pharyngeal marginal cells, gut, and several types of neurons. Moreover, SAGE shows that *mei-1* mRNA is also expressed in *glp-4* mutant adults.

To determine whether MEI-1 is the relevant target of MEL-26 in muscle, we examined the status of thick filaments in the striated muscle of adults in the *mei-1* gain-of-function allele, *ct46*, which encodes a protein that does not bind MEL-26 and so is resistant to MEL-26 mediated degradation (Clark-Maguire and Mains, 1994b; Pintard *et al.*, 2003; Xu *et al.*, 2003). This should correspond to the loss of *mel-26*. As shown in Figure 5B, *mei-1(ct46)* also shows disorganization of thick filaments, similar to loss of function of *mel-26*. This indicates that MEI-1 is a relevant target for the *mel-26* muscle phenotype.

To further explore the function of MEI-1 in striated muscle, we knocked down *mei-1* using RNAi feeding beginning from the L1 larval stage to bypass embryonic lethality. The resulting adults were immunostained with anti–MHC A, and the results are shown in Figure 5, C and D. Although there was some variation among animals in the severity of the phenotype, nearly all showed body-wall muscle cells in which thick filaments were disorganized. Cells showing the strongest effect resembled *unc-89* and *mel-26* mutants (compare bottom three panels of Figure 5C with Figure 4, A and B). To confirm the RNAi results for *mei-1*, we investigated the adult muscle phenotype of a null allele of *mei-1*, *ct46ct101* (Clark-Maguire and Mains, 1994a). We stained *mei-1*-mutant adult worms with anti–MHC A. As shown in Figure 5E, *mei-1(ct46ct101) unc-29(e1072)*, but not *unc-29(e1072)*, shows disorganization of thick filaments similar to that observed by RNAi for *mei-1*.

Therefore, *mei-1* gain of function and loss of function show similar phenotypes, as did gain and loss of function of *mel-26*, suggesting that tight regulation of the level of MEI-1 and MEL-26 is required for normal organization of thick filaments. An additional aspect of the phenotype can be noted: even in muscle cells showing a mild effect on thick-filament organization, the muscle cells appear shorter and broader than the narrower, spindle-shaped cells in wild-type muscle (Figure 5D). This effect on cell shape might be attributable to a disruption in the organization of microtubules that might result from the loss of MEI-1 or katanin activity.

Although MEI-1 has established microtubule-severing activity in *C. elegans* embryos, we sought genetic evidence for this function in

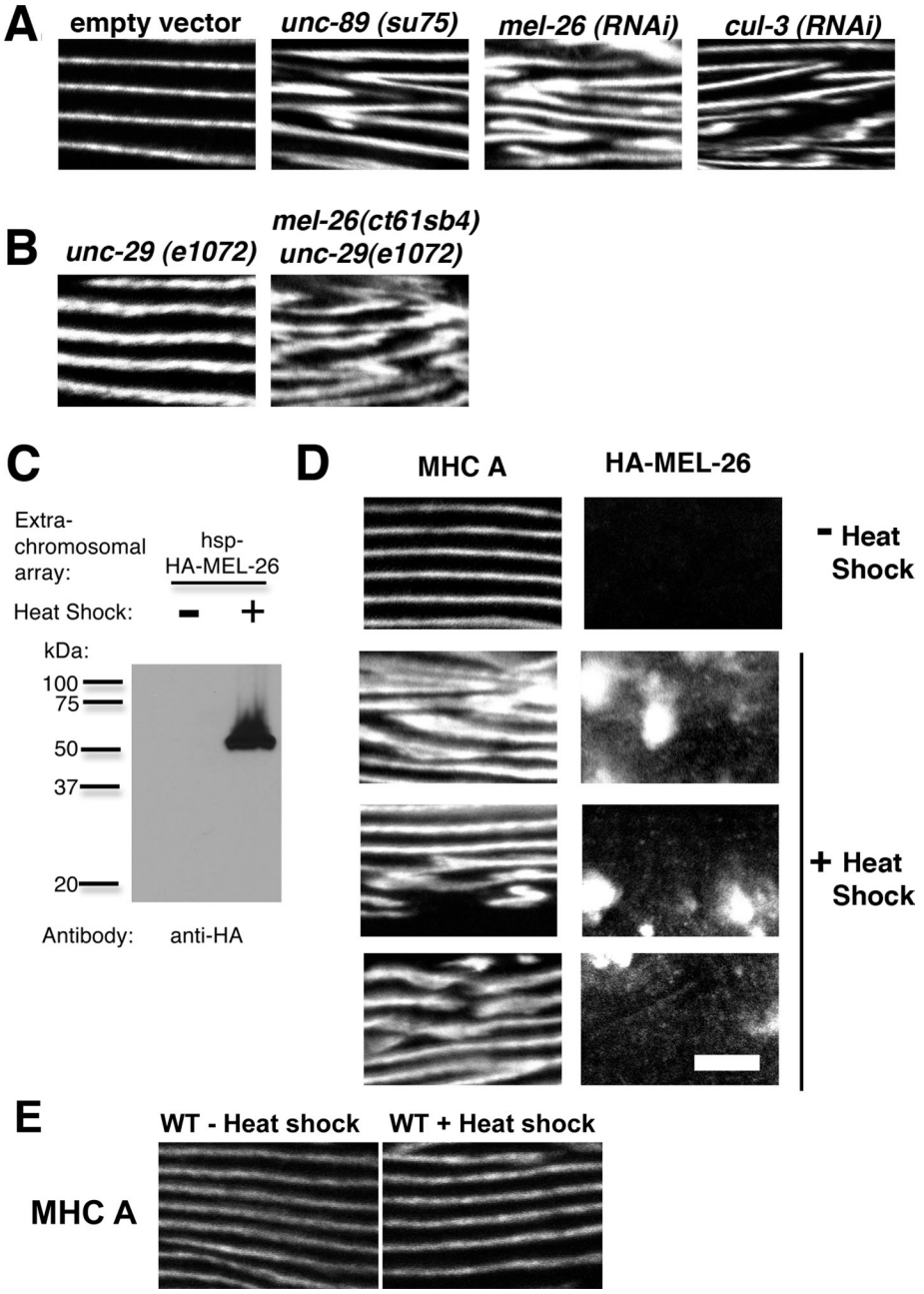

FIGURE 4: Loss of function or gain of function of *mel-26* and loss of function of *cul-3* result in myosin thick-filament disorganization similar to that found in *unc-89(su75)*. Images (except in C) show a portion of one body-wall muscle cell. (A) L1-stage transgenic animals expressing GFP::MHC A were fed bacteria carrying empty vector or vectors expressing double strand RNA for *mel-26* or *cul-3*. The resulting young adult worms were imaged for GFP::MHC A by confocal microscopy. For comparison, an image of GFP::MHC A in *unc-89(su75)* is shown. Note that *mel-26(RNAi)* gives a phenotype similar to *unc-89(su75)*, but that *cul-3(RNAi)* gives a phenotype more severe than *unc-89(su75)*. (B) The indicated strains were immunostained with anti-MHC A antibodies. *mel-26(ct61sb4)* is a null allele, and is marked with the neuronal Unc, *unc-29(e1072)*, which by itself shows normal thick-filament organization (left). *unc-29* was used as an aid in strain construction; see *Materials and Methods*. (C) Western blot of nematode lysates before and after heat shock of a transgenic line carrying an extrachromosomal array of HA-tagged MEL-26 under the control of a heat shock promoter. Only after heat shock can a protein of expected size be detected with anti-HA antibodies. (D) Images of portions of body-wall muscle from three different worms that showed significant HA-MEL-26 expression induced by heat shock. Left, MHC A immunostaining; right, the HA staining corresponding to MEL-26 overexpression and aggregation. Note the disorganization of thick filaments upon MEL-26 overexpression. (E) MHC A staining of wild-type muscle with and without heat shock. Note that heat shock itself had no effect on the organization of thick filaments. Bar, 5 μm.

body-wall muscle. To do this, we used nematode strains in which β-tubulin (TBB-2) contains a missense mutation that makes microtubules partially resistant to MEI-1 severing (Lu *et al.*, 2004). As shown in Figure 6 (bottom), this mutation, *tbb-2(sb26)*, by itself has no effect on the organization of thick filaments. However, the double mutant *mel-26(ct61sb4); tbb-2(sb26)* (Figure 6, middle) is partially suppressed as compared with *mel-26(ct61sb4)*. This indicates that at least some of the *mel-26* loss-of-function muscle phenotype can be attributed to increased microtubule-severing activity of MEI-1.

unc-89 influences proteasomal MEI-1 degradation

The fact that loss of function of *cul-3* or *mel-26* yields a similar phenotype to a gain-of-function allele of *mei-1* is consistent with the known biochemical function of the MEL-26/CUL-3 complex to degrade MEI-1 in early embryos (Furukawa *et al.*, 2003; Pintard *et al.*, 2003; Xu *et al.*, 2003). Therefore we hypothesize that the function of the UNC-89–MEL-26 interaction in adult muscle is to influence the activity of the MEL-26/CUL-3 complex in promoting the degradation of MEI-1. As a test of this hypothesis, we compared the level of MEI-1 protein in wild type versus *unc-89(su75)*. As noted earlier, *unc-89(su75)* lacks all UNC-89 isoforms that contain one of two MEL-26 binding sites. As shown in Figure 7A and quantitatively displayed in Figure 7C, *unc-89(su75)* shows a moderate reduction in the level of MEI-1 proteins. This is in contrast to the levels of PAT-6 (Figure 7A) or MHC A (Figure 7B), which show no difference between wild type and *unc-89(su75)*. PAT-6 is the nematode orthologue of actopaxin or α-parvin (Lin *et al.*, 2003) and is located at the base of muscle focal adhesions (M-lines and dense bodies). That we observed only a 20% reduction in the level of MEI-1 in *unc-89(su75)* might be explained by the facts that the animals analyzed were gravid adults and MEI-1 is expressed in early embryos and in multiple adult somatic tissues, whereas UNC-89 is almost exclusively expressed in body-wall and pharyngeal muscle. In addition, in *su75* animals the small UNC-89 isoforms C and D, which contain the second MEL-26–binding site, Ig53 and Fn2, are still expressed and, indeed, overexpressed as compared with wild type (Small *et al.*, 2004). However, RNAi of the interkinase region in the *unc-89(su75)* strain did not show a greater decrease of MEI-1 than *unc-89(su75)* alone, despite the fact that this RNAi of wild type resulted in thick-filament disorganization similar to that found in

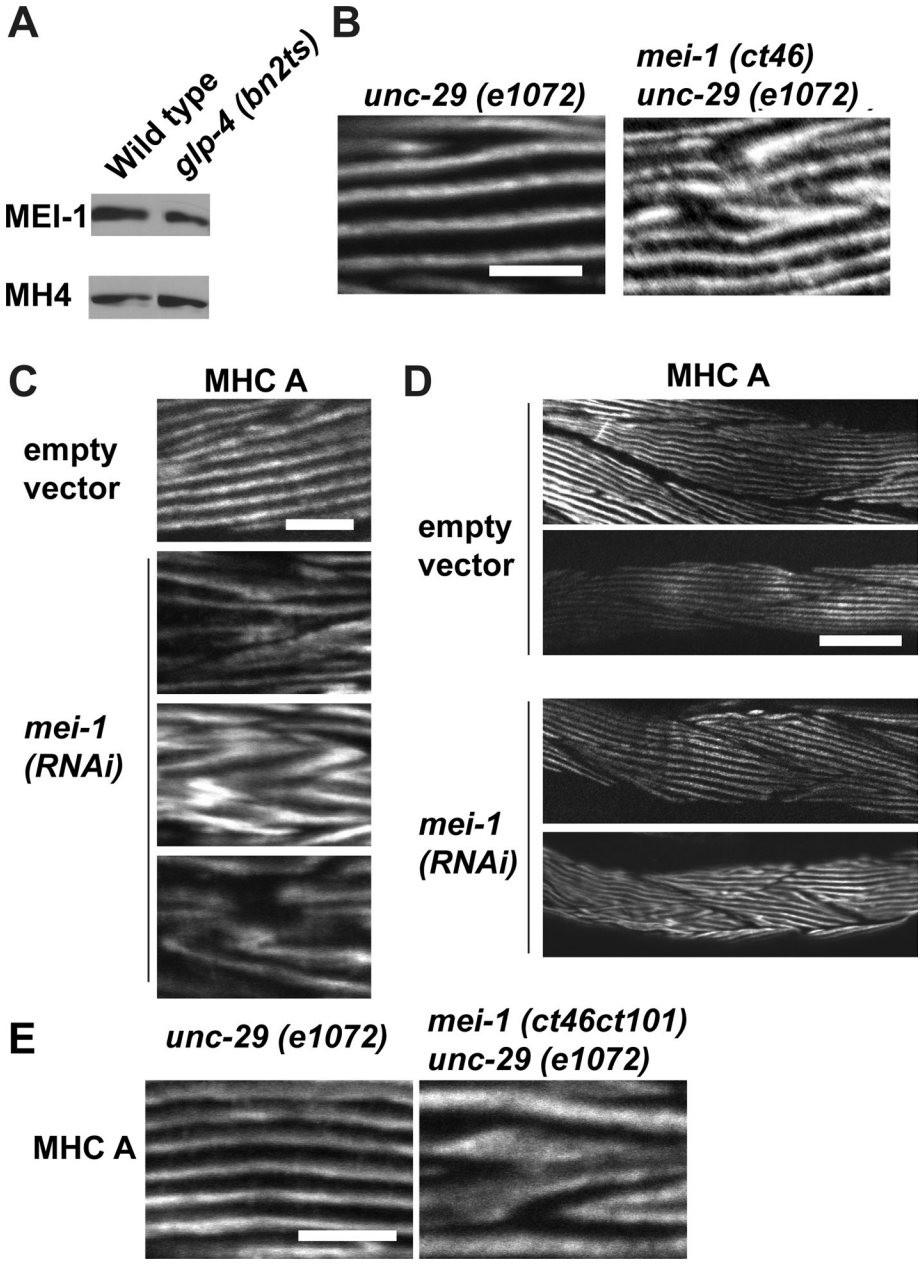

FIGURE 5: MEI-1 (katanin) is expressed in somatic cells, and both gain of function and loss of function of *mei-1* result in thick-filament disorganization similar to loss of function of *unc-89* and *mel-26*. (A) Western blot shows that MEI-1, a closely spaced doublet of ~50 kDa, can be detected in *glp-4(bn2ts)* animals, which lack a germline. Reaction to an intermediate filament protein (~70 kDa) expressed in hypodermal cells and detected with monoclonal antibody MH4 is shown as a loading control. (B) The indicated strains were immunostained with anti–MHC A antibodies. *mei-1(ct46)* is a gain-of-function allele refractory to *mel-26* inhibition and is marked with the neuronal Unc, *unc-29(e1072)*, which by itself shows normal thick-filament organization. *unc-29* was used as an aid in strain construction; see *Materials and Methods*. (C, D) RNAi by feeding beginning at the L1 stage was performed for *mei-1* (or with empty vector), and the resulting adults were immunostained with anti–MHC A. (C) Three representative examples of myosin staining from *mei-1(RNAi)* animals. Note that *mei-1(RNAi)* results in disorganization of thick filaments similar to loss of function of *unc-89* or gain or loss of function of *mel-26*. Bar, 5 μm. (D) Lower-magnification view (as compared with C), showing several body-wall muscle cells per field. Note that *mei-1(RNAi)* results in the body-wall muscle cells appearing shorter and broader as compared with wild type (empty vector). (E) The indicated strains were immunostained with anti–MHC A antibodies. *mei-1(ct46ct101)* is a null allele. As shown, the null state for *mei-1* results in thick-filament disorganization similar to knockdown of *mei-1* by RNAi (compare to C). Bars, 20 μm.

unc-89(tm752) (unpublished data), which shows a lack of expression of UNC-89-C and -D (Ferrara *et al.*, 2005). Nevertheless, a reduced level of MEI-1 in *unc-89(su75)* is consistent with a model in which the interaction of UNC-89 with MEL-26 normally functions to inhibit the activity of the CUL-3/MEL-26 complex in degrading muscle MEI-1 (see Figure 9 later in the paper).

Although MEI-1 has been shown to be ubiquitinated by CUL-3 in vitro (Furukawa *et al.*, 2003), it has not been reported whether this results in proteasomal degradation. RNAi against the proteasomal subunit RPT-2 (26S proteasome regulatory subunit 4) has been used to inhibit *C. elegans* proteasome function (Landsverk *et al.*, 2007). We performed RNAi against *rpt-2*, beginning at the L1 stage to avoid embryonic lethality, and prepared a protein extract. As compared with nematodes fed the empty RNAi vector, *rpt-2(RNAi)* led to an increased level of MEI-1 by Western blot (Figure 7, D and E). This result suggests that ubiquitination of MEI-1 leads to proteasomal degradation of MEI-1 in vivo.

Because loss of function of *unc-89* results in a lower level of MEI-1 (Figure 7), this suggests that normally UNC-89 inhibits its MEL-26 function. Given that UNC-89 and MEI-1 bind to the same domain of MEL-26 (the MATH domain; Figures 1D and 2B), one hypothesis is that UNC-89 and MEI-1 compete for binding to MEL-26. To test this possibility, we conducted the following experiment. Anti-HA beads were used to immunoprecipitate HA-MEL-26 (driven by a heat shock promoter) from lysates and incubated with no additional protein, maltose-binding protein (MBP), MBP-UNC-89 Ig2–Ig3, or MBP-UNC-89 Ig53–Fn2. As shown in Figure 8, although HA-MEL-26 coprecipitated native MEI-1, the presence of these additional proteins had no effect on this MEL-26–MEI-1 interaction. In fact, the HA-MEL-26 also interacted with the added MBP-Ig2-Ig3 and MBP-Ig53-Fn2 but not MBP. (There was some binding of MBP-Ig2-Ig3 and MBP-Ig53-Fn2 to the anti-HA beads, but this was considerably less than binding to HA-MEL-26–coated anti-HA beads.) These results indicate that either MEI-1 and UNC-89 bind nonoverlapping regions of MEL-26 MATH domain or MEI-1 binding is much stronger than that of UNC-89. Therefore, although we could find no evidence for competition in binding for MEL-26, MEL-26 activity may be influenced by interaction with UNC-89 in other ways (Figure 9; see *Discussion*).

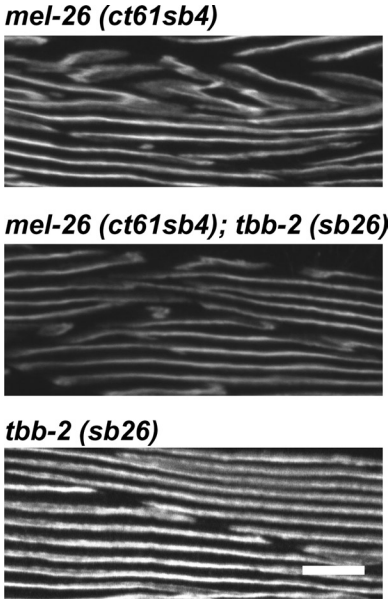

FIGURE 6: A β-tubulin mutant that is resistant to severing by MEI-1 partially suppresses the thick-filament disorganization of *mel-26*. The indicated strains were immunostained with anti–MHC A and imaged by confocal microscopy. Thick-filament organization of the β-tubulin mutant *tbb-2(sb26)* appears like that of wild type. Note the improvement in thick-filament organization in *mel-26(ct61sb4); tbb-2(sb26)* as compared with *mel-26(ct61sb4)*.

DISCUSSION

In our quest to identify binding partners for the giant sarcomeric protein UNC-89 (obscurin), we found that two portions of UNC-89 interact with the MEL-26, a BTB–domain containing substrate recognition protein known to interact with CUL-3 (Cul3)-based E3 ubiquitin ligase. Furthermore, we found that interaction of UNC-89 with MEL-26 occurs through the MATH domain of MEL-26 (Figures 1 and 2), the same domain of MEL-26 that had been identified previously as interacting with a known substrate of the CUL-3/MEL-26 complex in *C. elegans* embryos, the MEI-1 microtubule-severing protein (katanin). Using antibodies, we found that muscle MEL-26 is localized to M-lines, colocalizing with UNC-89, and to I-bands (Figure 3). To our knowledge this is the first time that a cullin-associated protein or a cullin has been localized in the sarcomere. Loss of function of *unc-89* results in a characteristic pattern of disorganization of muscle thick filaments, including myosin aggregates, which suggests a role for *unc-89* in thick-filament assembly and/or maintenance. We found that loss or gain of function of *mel-26* or loss of function or gain of function of *mei-1* results in thick-filament disorganization similar to that of *unc-89* loss of function (Figures 4 and 5). Because a mutant β-tubulin that is resistant to cleavage by MEI-1 (katanin) can partly suppress the thick-filament disorganization of a *mel-26* mutant (Figure 6), at least one function of MEI-1 in muscle is to sever microtubules. We observed that loss of function of *unc-89* results in a reduction in the level of MEI-1 protein (Figure 7, A–C). MEI-1, previously reported to be ubiquitinated in vitro, is likely to be degraded in the proteasome based on inhibiting proteasome function by *rpt-2(RNAi)* (Figure 7, D and E). However, compensating for decreased levels of MEI-1 caused by *unc-89* by inhibiting the proteasome did not improve the organization of thick filaments in *unc-89(su75)* versus *unc-89(su75); rpt-2(RNAi)* (unpublished data). This is consistent with our observations that *rpt-2(RNAi)* in the *unc-89*-mutant background still resulted in a rise of MEI-1 beyond wild-type levels and that gain of function of MEI-1 (Figure 5B) causes disorganization of thick filaments, as does MEI-1 loss of function.

To account for our findings, we propose a model in which the CUL-3/MEL-26 complex is localized to the M-line through the interaction of UNC-89 with MEL-26, and the function of this interaction is to inhibit ubiquitin-mediated degradation of MEI-1 (Figure 9). Given that both UNC-89 and MEI-1 bind to the MATH domain of MEL-26, we tested the hypothesis that UNC-89 and MEI-1 compete for binding to MEL-26. However, we could not demonstrate release of MEI-1 from MEL-26 in the presence of excess UNC-89 fragments (Figure 8). We could show that both MEI-1 and UNC-89 bound to MEL-26, but we do not know whether a single MEL-26 molecule can simultaneously bind to both MEI-1 and UNC-89 (e.g., using opposite surfaces of the MATH domain). Nevertheless, although there may not be direct competition for binding, the interaction of UNC-89 influences the activity of the CUL-3/MEL-26 complex toward MEI-1 and, given our data, most likely by inhibiting its activity. At the very least, the interaction of UNC-89 with MEL-26 localizes the activity of the CUL-3/MEL-26 complex at the sarcomeric M-line.

If our model that UNC-89 inhibits the complex is correct, then normally the activity of MEL-26 is reduced and the protein level of MEI-1 is elevated. Thus the similarity in phenotypes for loss of function of *unc-89*, for gain of function of *mel-26*, and for loss of function of *mei-1* is consistent with the model. The fact that we observed that both gain and loss of function of *mei-1* are also similar to loss of function of *unc-89* is more difficult to explain. Perhaps proper thick-filament assembly and/or maintenance depend on tightly controlled activities of *mei-1*, restricting it to a certain range of activity. This idea is not unprecedented: proper thick-filament assembly/maintenance is known to depend on precise levels of UNC-96 and UNC-45, as loss or gain of function of each gene results in similar effects on thick-filament organization (Barral *et al.*, 1998; Mercer *et al.*, 2006; Landsverk *et al.*, 2007; Qadota *et al.*, 2007). During meiosis, *mei-1* activity must also be kept within a specific range. Increased or decreased *mei-1* activity results in defective meiotic spindles, too short for increased activity or too long for decreased activity. In both cases, these abnormal spindles missegregate chromosomes, resulting in aneuploid gametes (Johnson *et al.*, 2009).

We also found that loss of function of *cul-3* results in a somewhat more severe disorganization of thick filaments than *unc-89*, *mel-26* or *mei-1* (Figure 4A). This perhaps suggests that in body-wall muscle, CUL-3 can associate with additional BTB adaptor proteins besides MEL-26. Indeed, our analysis reveals that the *C. elegans* genome contains 49 BTB domain–containing proteins. By SAGE data (on WormBase), 20 of the 49 are expressed in body-wall muscle, four of these probably at a high level of expression (including *mel-26*).

The ability of *tbb-2(sb26)* to partly suppress the thick-filament disorganization of *mel-26* is consistent with β-tubulin being at least one substrate for MEI-1 in muscle. However, since the phenotype is not entirely suppressed, there is the possibility that there may be additional substrates for MEI-1 muscle. Indeed, in the embryo the preference of MEI-1 for the TBB-2 β-tubulin isotype is not absolute (Lu *et al.*, 2004) and muscle may express additional tubulin isotypes. In addition, other MEI-1 functions, such as microtubule bundling (McNally and McNally, 2011), might be relevant in muscle. Nevertheless, we observed an additional aspect of the *mei-1(RNAi)* phenotype that is consistent with a role for microtubules in striated muscle: the spindle-shaped body-wall muscle cells are shorter in two dimensions. Disruption of the microtubule network in these cells may lead to a change in cell shape either during development or as a result of hypercontraction.

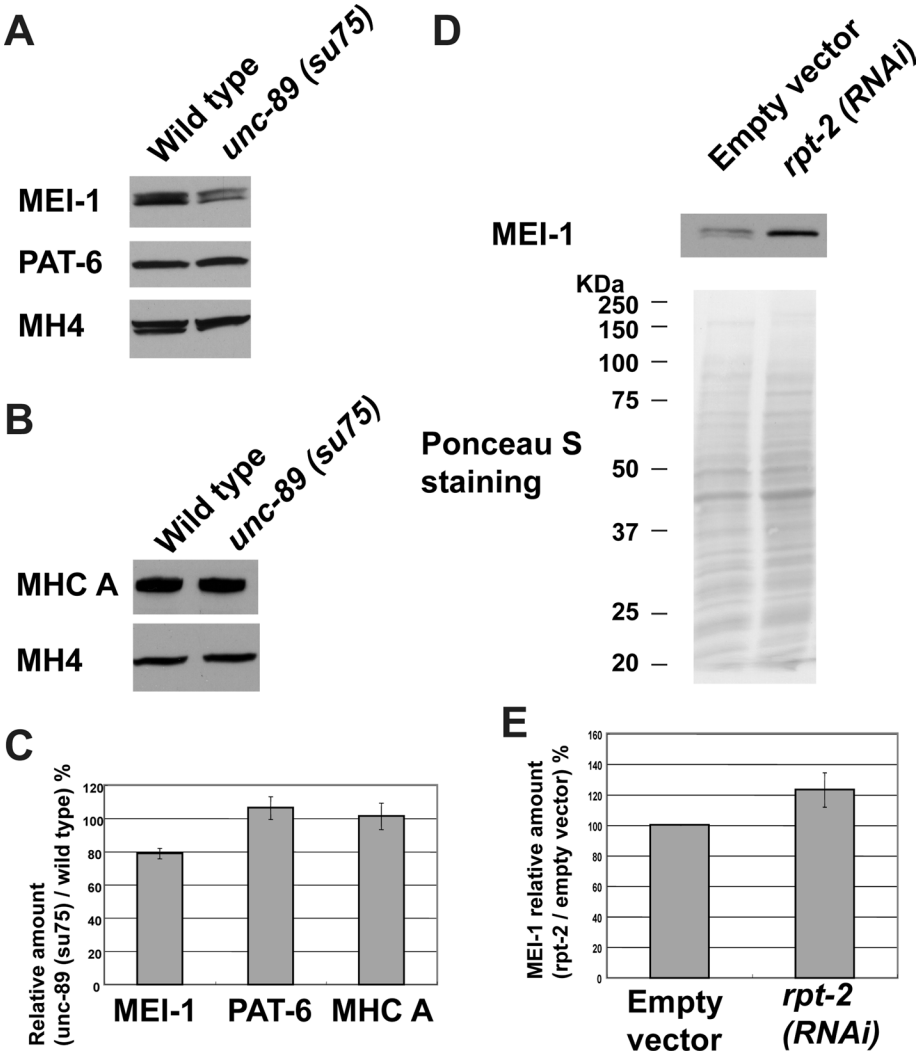

FIGURE 7: *unc-89* mutants have lower levels of MEI-1, and MEI-1 is degraded by the proteasome. (A) Equal quantities of Laemmli-soluble proteins from wild-type and *unc-89(su75)* strains were separated by a 10% SDS–PAGE, transferred to membrane, and reacted with antibodies to MEI-1, PAT-6, and the monoclonal MH4. In *unc-89(su75)*, the level of MEI-1 is reduced, whereas the level of PAT-6 (~41 kDa) is unchanged (quantitated in C). (B) Equal quantities of Laemmli-soluble protein from wild-type and *unc-89(su75)* strains were separated by 7.5% SDS–PAGE, transferred to membrane, and reacted with antibodies to MHC A and the monoclonal MH4. In *unc-89(su75)*, the level of MHC A is unchanged. (C) Graphical representation of results shown in A and B. The experiment shown in A was repeated three times; that in B, twice. For each lane, the quantity of MEI-1, PAT-6, and MHC A was divided (or normalized) by the quantity of MH4 from that lane. For each pair of lanes (*unc-89* and wild type), the normalized quantity from *unc-89* was divided by the normalized quantity from wild type and multiplied by 100. The mean and SD of these numbers are represented for each protein in the bars. Note that in *unc-89(su75)*, there was a 20% reduction in the level of MEI-1 but no significant change in the levels of PAT-6 or MHC A. (D) Western blot using anti–MEI-1 comparing equal quantities of Laemmli-soluble proteins from nematodes fed bacteria harboring the RNAi empty vector and the *rpt-2(RNAi)* plasmid. Below are images of the blot stained with Ponceau S before reaction with anti–MEI-1. (E) Quantitation of results depicted in D. The means and SDs from three experiments are represented. Because the level of each protein examined (including the protein detected by MH4) was elevated by *rpt-2 (RNAi)*, we normalized by total Ponceau S protein from the blot strips.

Little is known about the potential role of microtubules in muscle cell shape or sarcomeric organization in *C. elegans*. To our knowledge, the localization of microtubules in nematode body-wall muscle has not been reported. Nevertheless, the *C. elegans* echinoderm microtubule-associated protein–like protein ELP-1, which binds to microtubules in vitro, is localized in a criss-crossing network resembling microtubules, and the network is sensitive to the microtubule disruptor nocodazole (Hueston *et al.*, 2008). Of interest, RNAi-mediated knockdown of *elp-1* in a dystrophin (*dys-1*)-null animal results in adult worms that have hypercontracted muscle cells (Hueston and Suprenant, 2009), similar to what we observed for *mei-1(RNAi)*. In mammals, electron microscopy of cardiac muscle revealed a fairly extensive network of microtubules; microtubules surround myofibrils and sarcoplasmic reticulum in a helical arrangement (Goldstein and Entman, 1979). In myotubes induced to regenerate their myofibrils, in the presence of the microtubule-stabilizing drug Taxol, A-bands are formed, but thin filaments and Z-bands are not formed; in the presence of the microtubule-depolymerizing drug Colcemid, complete sarcomeres are formed, but they are not laterally aligned (Toyama *et al.*, 1982). Generation of a stable, postranslationally modified microtubule array is an early event in the differentiation of myotubes (Gundersen *et al.*, 1989). During cardiac hypertrophy, there is an increase in microtubule network density associated with sarcomere dysfunction (Tsutsui *et al.*, 1993).

The results presented here are not the first to implicate the ubiquitin proteasome system in controlled degradation of sarcomeric proteins in *C. elegans*. The RING finger protein RNF-5, not known to be associated with cullins, is localized to dense bodies (Z-disks) and regulates the levels of the LIM domain protein UNC-95 (Broday *et al.*, 2004). A report from our laboratory demonstrated a connection to CRLs. We showed that CSN-5 interacts with two sarcomeric M-line proteins, UNC-98 and UNC-96 (Miller *et al.*, 2009). CSN-5 is one of eight highly conserved subunits of the COP9 signalosome complex, which regulates CRLs in a complicated manner, primarily through deneddylation (Cope and Deshaies, 2003; Schwechheimer, 2004). Antibodies to CSN-5 localize the protein to A-bands in wild type and colocalize with abnormal accumulations of paramyosin found in *unc-98*, *unc-96*, and *unc-15* (paramyosin) mutants. Knockdown of *csn-5* results in an increase in the level of UNC-98 protein and a slight reduction in the level of UNC-96 protein, suggesting that normally CSN-5 promotes the degradation of UNC-98 and stabilizes UNC-96.

Cullins and BTB-domain proteins are associated with human diseases. Litterman *et al.* (2011) reported that in humans, obscurin-like 1 (OBSL1) directly interacts with Cul7, and both proteins are crucial for Golgi morphogenesis and dendrite growth of neurons. Cul7 and OBSL1 also cause human 3M syndrome, an

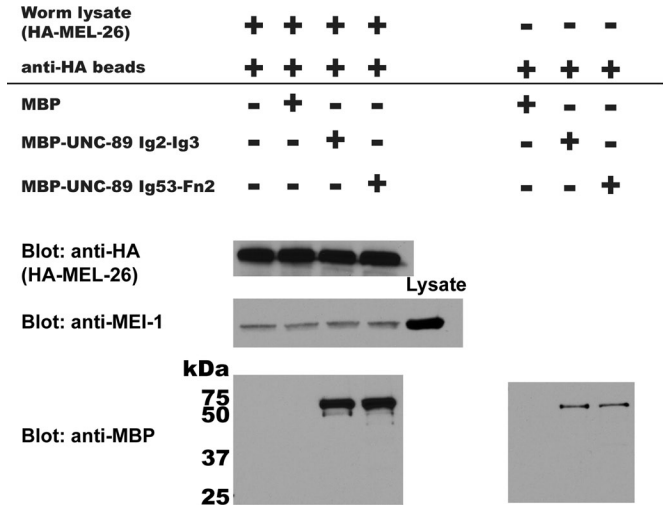

FIGURE 8: Recombinant UNC-89 fragments do not release native MEI-1 bound to HA-MEL-26. A lysate was prepared from a nematode strain with integrated HA-MEL-26 driven by a heat shock promoter after heat shock. HA-MEL-26 was pelleted using anti-HA beads and incubated with MBP, MBP-Ig2-Ig3, or MBP-Ig53-Fn2 and pelleted, and the resulting proteins were analyzed by Western blot using specific antibodies to the indicated proteins. Note that the presence of the added proteins did not release MEI-1 that was previously bound to HA-MEL-26–coated beads and that these beads also bound MBP-Ig2-Ig3 and MBP-Ig53-Fn2 (bottom left). Right, a control experiment indicating that some MBP-Ig2-Ig3 and MBP-Ig53-Fn2 could bind to uncoated anti-HA beads, albeit much in lower amounts than for beads coated with HA-MEL-26 (the same exposure time in the ECL reaction was used for both blots in which anti-MBP was used).

autosomal recessive disorder characterized by growth retardation, characteristic facial features, and skeletal anomalies. The majority of patients have mutations in Cul7, whereas others have null mutations in OBSL1 (Hanson *et al.*, 2009). Cirak *et al.* (2010) reported a family in which early-onset autosomal-dominant distal myopathy is associated with a heterozygous missense mutation in Kelch-like homologue 9 (KLHL9), which is a substrate recognition protein that interacts with Cul3. Of interest, the mutation, L95F, is located in the conserved BTB domain of KLHL9, which mediates interaction with Cul3.

Finally, in Lange *et al.* (2012), our colleagues studying obscurin in the mammalian heart show that the turnover of the small ankyrin protein sAnk1.5, previously known to interact with obscurin, is regulated by ubiquitylation mediated by the BTB-domain protein KCTD6. KCTD6, like MEL-26, is a substrate recognition protein for Cul3. Furthermore, these authors demonstrate that in the absence of obscurin, degradation of sAnk1.5 is increased, and conversely, RNAi-mediated knockdown of KCTD6 results in increased levels of sAnk1.5. Thus, although the ultimate substrates identified by our study and that of Lange *et al.* are different—MEI-1 and sAnk1.5, respectively—the mechanism is similar: apparent inhibition of a Cul3 complex in striated muscle by UNC-89 (obscurin).

MATERIALS AND METHODS

Plasmid construction

To construct plasmids for yeast two-hybrid assays and other purposes, we amplified the various portions of UNC-89, MEL-26, CUL-3, and MEI-1, as depicted in Figure 1, as well as RPT-2 (boundaries of constructs, primer sequences, and enzymes used are shown in Supplemental Tables S1 and S2). After cloning into pBluescript and verifying error-free sequences, we subcloned the fragments into the bait vector pGBDU-C1 and/or the prey vector pGAD-C1 (James *et al.*, 1996). In addition, the DNA fragments were subcloned into pGEX-KK1 and/or pMAL-KK1 (kindly provided by Kozo Kaibuchi, Nagoya University, Nagoya, Japan) for the purification of glutathione *S*-transferase (GST)- or MBP-tagged proteins, respectively. Similarly, sequences were subcloned into pPD129.36 for RNAi or into pKS-HA8(NheX2) to add HA tag to the N-terminus and then into nematode heat shock promoter vectors pPD49.78 and pPD49.83 (gifts from Andrew Fire, Stanford University, Stanford, CA).

Yeast two-hybrid assays and bookshelf screens

Yeast two-hybrid assays were performed as previously described (Mackinnon *et al.*, 2002). Briefly, PJ69-4A strains carrying pGBDU bait constructs were transformed with prey clones (using either pACT or pGAD vectors). Assays were scored for growth on media lacking either histidine or adenine. MEL-26 was used as bait to screen a collection ("bookshelf") of 16 overlapping sequences that cover all of the coding sequence of the largest isoform of UNC-89 (Xiong *et al.*, unpublished data). Deletion derivatives of UNC-89 Ig1–5, IK–Fn2, and MEL-26, as depicted in Figure 1 and Supplemental Table S2, were tested by two-hybrid assay in a similar manner.

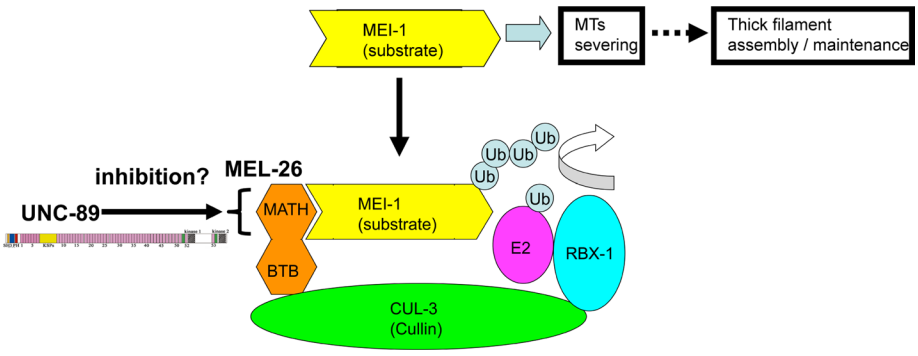

FIGURE 9: Model of the interactions among UNC-89, MEL-26, and MEI-1 in striated muscle. UNC-89 interacts with the MATH domain of MEL-26 at sarcomeric M-lines and is likely to inhibit the activity of the CUL-3/MEL-26 complex from promoting the ubiquitin-mediated degradation of MEI-1. Normally, MEI-1 severs microtubules, and this activity is in some manner required for thick-filament assembly and/or maintenance.

Purification of bacterially expressed proteins and demonstration of interactions using purified proteins

Bacterially expressed GST- and MBP-tagged proteins were purified as previously described (Mercer *et al.*, 2006). Far Western assays were used to verify interactions using purified proteins as previously described (Qadota *et al.*, 2007). Briefly, 2 µg of GST or GST-tagged proteins were resolved by SDS–PAGE and electroblotted onto nitrocellulose. Blots were then reacted with 5 µg/ml MBP or MBP-tagged proteins. MBP binding was detected by a 1:5000 dilution of anti-MBP (mouse monoclonal)–horseradish peroxidase (HRP; E8038S; New England BioLabs, Ipswich, MA) and visualized using

enhanced chemiluminescence (ECL; 32106; Pierce, Thermo Fisher Scientific, Rockford, IL).

C. elegans strains and culture

The wild-type strain, Bristol N2, strain RW1596 (see later discussion), HE75 (*unc-89(su75)*, originally isolated and provided by Henry Epstein, University of Texas Medical Branch at Galveston, Galveston, TX; Small *et al.*, 2004), CB1072 (*unc-29(e1072)*; Lewis *et al.*, 1980), HR1060 (*tbb-2(sb26)*; Lu *et al.*, 2004), and HR311 (*mei-1(ct46ct101) unc-29(e1072)/hT2* [*bli-4(e937) let(h661)*] (I); *+/hT2* III; Johnson *et al.*, 2009) were grown at 20°C on nematode growth media (NGM) plates with *Escherichia coli* strain OP50 as food source (Brenner, 1974). The temperature-sensitive strains HR1329 (*mel-26(ct61sb4) unc-29(e1072)*; Lu and Mains, 2007), BW729 (*mei-1(ct46) unc-29(e1072)*; Clark-Maguire and Mains, 1994b), SS104 (*glp-4(bn2ts)*; Beanan and Strome, 1992), and HR1065 (*mel-26 (ct61sb4) unc-29(e1072); tbb-2(sb26)*; Lu *et al.*, 2004) were grown at 15°C. RW1596 is a *myo-3* mutant rescued by a transgenic array containing copies of the wild-type *myo-3* gene (encodes MHC A) translationally fused to GFP (Campagnola *et al.*, 2002) and provided by Pamela Hoppe (Western Michigan University, Kalamazoo, MI).

Because *mel-26* and *mei-1* do not have easily scorable adult phenotypes (other than by progeny testing), the closely linked marker gene on chromosome I, *unc-29*, which has a recognizable adult motility defect, was used to follow the presence of the mutant genes through genetic crosses (*unc-29* shows <1% recombination with either gene). *unc-29* encodes a non-α subunit of the nicotinic acetylcholine receptor superfamily and is expressed in body-wall muscle (Fleming *et al.*, 1997), but, as shown in Figures 4B and 5, B and E), loss of function does not affect sarcomeric structure.

Immunofluorescence microscopy

Worm fixation by the Nonet method and worm immunostaining were as previously described (Wilson *et al.*, 2012). In the case of *mei-1(ct46ct101)*, to collect homozygous adult worms, we used strain HR311 (in which *mei-1* is genetically marked by the closely linked *unc-29(e1072)*); we picked 200 Unc-29 worms (identified by reduced forward movement) for fixation. Primary antibodies were used at the following dilutions: 1:100 rabbit anti–MEL-26 (affinity purified; a generous gift from Lionel Pintard, University of Paris; Luke-Glaser *et al.*, 2007a), 1:200 mouse anti–UNC-89 (MH42; monoclonal, ascites) from Benian *et al.*, 1996), 1:200 mouse anti–α-actinin (MH35; monoclonal, ascites) from Francis and Waterston (1985)), 1:200 mouse anti–myosin heavy chain A (MHC A) (5-6; monoclonal, tissue culture supernatant) from Miller *et al.* (1983), and 1:200 mouse anti-HA monoclonal antibodies (H3663; Sigma-Aldrich, St. Louis, MO). Secondary antibodies and confocal microscopy were as described (Qadota *et al.*, 2007). The color balances of the images were adjusted with Photoshop (Adobe, San Jose, CA).

Analysis of muscle phenotypes by RNAi

RNAi of *mel-26*, *cul-3*, or *mei-1* was performed by feeding the specified worm strain bacteria expressing double-stranded RNA beginning at the L1 larval stage and continuing until the animals reached adulthood (Miller *et al.*, 2006). L1 larvae were isolated by performing a bleach/NaOH digestion of an unsynchronized worm culture resulting in only viable embryos. Embryos were plated on unseeded NGM plates overnight, allowing the L1 larvae to hatch but not grow. These synchronized L1 larvae were collected and distributed onto plates containing bacteria expressing double-stranded RNA. Plates were incubated for 2 d, and then adults were either examined for localization of GFP-MHC A by confocal microscopy or were fixed, immunostained with anti-MHC A, and examined by confocal microscopy. To examine the effect on the level of MEI-1 by knocking down a component of the proteasome, RPT-2, we conducted RNAi for *rpt-2* beginning at the L1 stage, as described earlier. In this case, embryos were harvested from a heavy growth of N2 from 10 10-cm plates and allowed to hatch into L1, and these L1 were grown into adults on 50 10-cm plates before harvesting for Western blot analysis.

Transgenic worms

Plasmids capable of expressing HA-tagged MEL-26 under the control of a heat shock promoter (described earlier) were coinjected with the SUR-5::NLS::GFP transformation marker plasmid pTG96 (Yochem *et al.*, 1998). F1 worms with GFP expression were cloned, and two lines were established (both lines behaved similarly; unpublished data). HA-MEL-26 expression was examined using worms with and without a 2-h heat shock at 30°C, preparing a worm lysate (Hannak *et al.*, 2002), and assaying by Western blot using rabbit anti-HA (H6908; Sigma-Aldrich). Worms were also treated with and without a 2-h heat shock at 30°C, allowed to recover at 20°C overnight, and then fixed and immunostained with anti-MHC A, as described previously.

Western blots and quantitation of protein levels

We used the procedure of Hannak *et al.* (2002) to prepare total protein lysates from wild-type, *glp-4(bn2ts)*, and *unc-89(su75)* strains. When comparing wild-type and mutant strains, we loaded approximately equal amounts of protein extract estimated by finding volumes of extracts that would give equal intensity of banding after Coomassie staining. We used quantities of extracts and dilutions of antibodies that would place us into the linear range of detection by ECL and exposure to film. The following antibodies and dilutions were used: rabbit anti–MEI-1 (affinity purified; Clark-Maguire and Mains, 1994b) at 1:400; rat anti–PAT-6 (affinity purified; Xiong *et al.*, unpublished data) at 1:200; monoclonal MH4 (tissue culture supernatant; Francis and Waterston, 1985), which detects intermediate filaments expressed in hypodermal cells at 1:1000; and monoclonal 5-6 (Miller *et al.*, 1983) for MHC A at 1:1000. The specificities of all antibodies used in this study were established previously (see the respective references cited earlier). The quantitation of steady-state levels of MEI-1, PAT-6, and MHC A shown in Figure 7C was performed as described in Miller *et al.* (2009). The relative amount of each of these muscle proteins in each lane was normalized to the amount of MH4 antigen.

Attempt to release MEI-1 from MEL-26 using portions of UNC-89

An extrachromosomal array containing pPD49.78/83-HA-MEL-26 and pTG96 was integrated into the genome by UV irradiation (Mitani, 1995) with some modifications (P. Barrett, personal communication). The resulting integrated nematode line is called *sfIs8* and was grown on 20 150-mm high-peptone plates seeded with NA22 *E. coli* and heat shocked for 3 h at 30°C. The worms were harvested and washed in M9 buffer, frozen at −80°C, and used to prepare a powder by extensive grinding with a mortar and pestle sitting on dry ice and the worms immersed in liquid nitrogen. A lysate was prepared by vortexing for 2 min a 10% (vol/vol) mixture of worm powder in lysis buffer (20 mM Tris, pH 8.0, 10% glycerol, 0.5% NP-40, 2 mM EDTA, 150 mM NaCl, complete Mini Protease Inhibitors [Roche, Indianapolis, IN]) spinning at top speed in a microcentrifuge for 10 min at 4°C and saving the supernatant. Four separate Eppendorf tubes contained 500 µl of worm lysate, and 50 µl of a

1:1 (vol/vol) slurry of monoclonal anti–HA-agarose beads (A2095; Sigma-Aldrich) was incubated with mixing at 4°C for 1.5 h. After washing the beads three times with lysis buffer, 20 µg of the following proteins were added separately: MBP, MBP-UNC-89 Ig2–Ig3, and MBP-UNC-89 Ig53–Fn2. The solutions were incubated with mixing at 4°C for 1.5 h. After washing the beads three times with lysis buffer, the beads were transferred to fresh tubes, pelleted, and eluted with Laemmli buffer at 95°C for 5 min and pelleted, and portions of supernatants were run on SDS–PAGE and blotted. One blot was used to detect MEI-1 (using affinity-purified rabbit anti–MEI-1 at 1:400 dilution) and MBP or MBP fusion proteins (using anti-MBP conjugated to HRP at 1:5000 dilution). Another blot was used to detect HA-MEL-26 (using anti-HA [mouse monoclonal] at 1:200 dilution). A control experiment was set up in which anti–HA-agarose beads were incubated with 20 µg of MBP, MBP-UNC-89 Ig2–Ig3, and MBP-UNC-89 Ig53–Fn2, washed, and eluted, and the MBP and MBP fusion proteins were detected by Western blot.

ACKNOWLEDGMENTS

We thank Stephan Lange (University of California, San Diego, La Jolla, CA) for helpful discussions and for communicating his results before their publication. We are grateful to Lionel Pintard (University of Paris) for supplying the antibody to MEL-26, and we thank Andrew Fire (Stanford University) for RNAi and heat shock promoter vectors. G.M.B. thanks the Department of Pathology and School of Medicine of Emory University for bridge funds. We also acknowledge a Fellowship in Research and Science Teaching Postdoctoral Fellowship (K12GM000680) from the National Institutes of Health (for K.J.W.) and support from National Institutes of Health Grant R01AR051466. P.E.M. was supported by a grant from the Canadian Institutes of Health Research. Some of the strains used in this work were provided by the *Caenorhabditis* Genetics Center (funded by the National Institutes of Health, Center for Research Resources).

REFERENCES

Bang ML *et al.* (2001). The complete gene sequence of titin, expression of an unusual approximately 700-kDa titin isoform, and its interaction with obscurin identify a novel Z-line to I-band linking system. Circ Res 89, 1065–1072.

Barral JM, Bauer CC, Ortiz I, Epstein HF (1998). unc-45 mutations in *C. elegans* implicate a CRO1/She4p-like domain in myosin assembly. J Cell Biol 143, 1215–1225.

Beanan MJ, Strome S (1992). Characterization of a germ-line proliferation mutation in *C. elegans*. Development 116, 755–766.

Benian GM, Ayme-Southgate A, Tinley TL (1999). The genetics and molecular biology of the titin/connectin-like proteins of invertebrates. Rev Physiol Biochem Pharmacol 138, 235–268.

Benian GM, Epstein HF (2011). *Caenorhabditis elegans* muscle: a genetic and molecular model for protein interactions in the heart. Circ Res 109, 1082–1095.

Benian GM, Tinley TL, Tang X, Borodovsky M (1996). The *Caenorhabditis elegans* gene unc-89, required for muscle M-line assembly, encodes a giant modular protein composed of Ig and signal transduction domains. J Cell Biol 132, 835–848.

Bodine SC *et al.* (2001). Identification of ubiquitin ligases required for skeletal muscle atrophy. Science 294, 1704–1708.

Bosu DR, Kipreos ET (2008). Cullin-RING ubiquitin ligases: global regulation and activation cycles. Cell Div 3, 7.

Brenner S (1974). The genetics of *Caenorhabditis elegans*. Genetics 77, 71–94.

Broday L, Kolotuev I, Didier C, Bhoumik A, Podbilewicz B, Ronai Z (2004). The LIM domain protein UNC-95 is required for the assembly of muscle attachment structures and is regulated by the RING finger protein RNF-5 in *C. elegans*. J Cell Biol 165, 857–867.

Campagnola PJ, Millard AC, Terasaki M, Hoppe PE, Malone CJ, Mohler WA (2002). Three-dimensional high-resolution second-harmonic generation imaging of endogenous structural proteins in biological tissues. Biophys J 82, 493–508.

Cirak S *et al.* (2010). Kelch-like homologue 9 mutation is associated with an early onset autosomal dominant distal myopathy. Brain 133, 2123–2135.

Clark-Maguire S, Mains PE (1994a). *mei-1*, a gene required for meiotic spindle formation in *C. elegans*, is a member of a family of ATPases. Genetics 136, 533–546.

Clark-Maguire S, Mains PE (1994b). Localization of the mei-1 gene product of *Caenorhabditis elegans*, a meiotic-specific spindle component. J Cell Biol 126, 199–209.

Cope GA, Deshaies RJ (2003). COP9 signalosome: a multifunctional regulator of SCF and other cullin-based ubiquitin ligases. Cell 114, 663–671.

Dow MR, Mains PE (1998). Genetic and molecular characterization of the *C. elegans* gene, mel-26, a postmeiotic negative regulator of mei-1, a meiotic-specific spindle component. Genetics 150, 119–128.

Ferrara TM, Flaherty DB, Benian GM (2005). Titin/connectin-related proteins in *C. elegans*: a review and new findings. J Muscle Res Cell Motil 26, 435–447.

Fleming JT *et al.* (1997). *Caenorhabditis elegans* levamisole resistance genes *lev-1*, *unc-29*, and *unc-38* encode functional nicotinic acetylcholine receptor subunits. J Neurosci 17, 5843–5857.

Francis GR, Waterston RH (1985). Muscle organization in *Caenorhabditis elegans*: localization of proteins implicated in thin filament attachment and I-band organization. J Cell Biol 101, 1532–1549.

Fukuzawa A, Idowu S, Gautel M (2005). Complete human gene structure of obscurin: implications for isoform generation by differential splicing. J Muscle Res Cell Motil 26, 427–434.

Furukawa M, He YJ, Borchers C, Xiong Y (2003). Targeting of protein ubiquitination by BTB-cullin 3-Roc1 ubiquitin ligases. Nat Cell Biol 5, 1001–1007.

Goldstein MA, Entman ML (1979). Microtubules in mammalian heart muscle. J Cell Biol 80, 183–195.

Gomes MD, Lecker SH, Jagoe RT, Navon A, Goldberg AL (2001). Atrogin-1, a muscle-specific F-box protein highly expressed during muscle atrophy. Proc Natl Acad Sci USA 98, 14440–14445.

Gundersen GG, Khawaja S, Bulinski JC (1989). Generation of a stable, post-translationally modified microtubule array is an early event in myogenic differentiation. J Cell Biol 109, 2275–2288.

Hannak E, Oegema K, Kirkham M, Gonczy P, Habermann B, Hyman AA (2002). The kinetically dominant assembly pathway for centrosomal asters in *Caenorhabditis elegans* is gamma-tubulin dependent. J Cell Biol 157, 591–602.

Hanson D *et al.* (2009). The primordial growth disorder 3-M syndrome connects ubiquitination to the cytoskeletal adaptor OBSL1. Am J Hum Genet 84, 801–806.

Hueston JL, Herren GP, Cueva JG, Buechner M, Lundquist EA, Goodman MB, Suprenant KA (2008). The *C. elegans* EMAP-like protein, ELP-1 is required for touch sensation and associates with microtubules and adhesion complexes. BMC Dev Biol 8, 110.

Hueston JL, Suprenant KA (2009). Loss of dystrophin and the microtubule-binding protein ELP-1 causes progressive paralysis and death of adult *C. elegans*. Dev Dyn 238, 1878–1886.

James P, Halladay J, Craig EA (1996). Genomic libraries and a host strain designed for highly efficient two-hybrid selection in yeast. Genetics 144, 1425–1436.

Johnson JL, Lu C, Raharjo E, McNally K, McNally FJ, Mains PE (2009). Levels of the ubiquitin ligase substrate adaptor MEL-26 are inversely correlated with MEI-1/katanin microtubule-severing activity during both meiosis and mitosis. Dev Biol 330, 349–357.

Kontrogianni-Konstantopoulos A, Ackermann MA, Bowman AL, Yap SV, Bloch RJ (2009). Muscle giants: molecular scaffolds in sarcomerogenesis. Physiol Rev 89, 1217–1267.

Landsverk ML, Li S, Hutagalung AH, Najafov A, Hoppe T, Barral JM, Epstein HF (2007). The UNC-45 chaperone mediates sarcomere assembly through myosin degradation in *Caenorhabditis elegans*. J Cell Biol 177, 205–210.

Lange S, Perera S, Teh P, Chen J (2012). Obscurin and KCTD6 regulate cullin-dependent small ankyrin-1 (sAnk1.5) protein turnover. Mol Biol Cell 23, 2490–2504.

Lewis JA, Wu CH, Berg H, Levine JH (1980). The genetics of levamisole resistance in the nematode *Caenorhabditis elegans*. Genetics 95, 905–928.

Lin X, Qadota H, Moerman DG, Williams BD (2003). *C. elegans* PAT-6/actopaxin plays a critical role in the assembly of integrin adhesion complexes in vivo. Curr Biol 13, 922–932.

Litterman N, Ikeuchi Y, Gallardo G, O'Connell BC, Sowa ME, Gygi SP, Harper JW, Bonni A (2011). An OBSL1-Cul7Fbxw8 ubiquitin ligase signaling mechanism regulates Golgi morphology and dendrite patterning. PLoS Biol 9, e1001060.

Lu C, Mains PE (2007). The *C. elegans* anaphase promoting complex and MBK-2/DYRK kinase act redundantly with CUL-3/MEL-26 ubiquitin ligase to degrade MEI-1 microtubule-severing activity after meiosis. Dev Biol 302, 438–447.

Lu C, Srayko M, Mains PE (2004). The *Caenorhabditis elegans* microtubule-severing complex MEI-1/MEI-2 katanin interacts differently with two superficially redundant beta-tubulin isotypes. Mol Biol Cell 15, 142–150.

Luke-Glaser S, Pintard L, Tyers M, Peter M (2007a). The AAA-ATPase FIGL-1 controls mitotic progression, and its levels are regulated by the CUL-3 MEL-26 E3 ligase in the *C. elegans* germ line. J Cell Sci 120, 3179–3187.

Luke-Glaser S, Roy M, Larsen B, Le Bihan T, Metalnikov P, Tyers M, Peter M, Pintard L (2007b). CIF-1, a shared subunit of the COP9/signalosome and eukaryotic initiation factor 3 complexes, regulates MEL-26 levels in the *C. elegans* embryo. Mol Cell Biol 27, 4526–4540.

Machida K, Mayer BJ (2009). Detection of protein-protein interactions by far-Western blotting. Methods Mol Biol 536, 313–329.

Mackinnon AC, Qadota H, Norman KR, Moerman DG, Williams BD (2002). *C. elegans* PAT-4/ILK functions as an adaptor protein within integrin adhesion complexes. Curr Biol 12, 787–797.

McNally K, Audhya A, Oegema K, McNally FJ (2006). Katanin controls mitotic and meiotic spindle length. J Cell Biol 175, 881–891.

McNally KP, McNally FJ (2011). The spindle assembly function of *Caenorhabditis elegans* katanin does not require microtubule-severing activity. Mol Biol Cell 22, 1550–1560.

Mercer KB, Miller RK, Tinley TL, Sheth S, Qadota H, Benian GM (2006). *Caenorhabditis elegans* UNC-96 is a new component of M-lines that interacts with UNC-98 and paramyosin and is required in adult muscle for assembly and/or maintenance of thick filaments. Mol Biol Cell 17, 3832–3847.

Miller DM 3rd, Ortiz I, Berliner GC, Epstein HF (1983). Differential localization of two myosins within nematode thick filaments. Cell 34, 477–490.

Miller RK, Qadota H, Landsverk ML, Mercer KB, Epstein HF, Benian GM (2006). UNC-98 links an integrin-associated complex to thick filaments in *Caenorhabditis elegans* muscle. J Cell Biol 175, 853–859.

Miller RK, Qadota H, Stark TJ, Mercer KB, Wortham TS, Anyanful A, Benian GM (2009). CSN-5, a component of the COP9 signalosome complex, regulates the levels of UNC-96 and UNC-98, two components of M-lines in *C. elegans* muscle. Mol Biol Cell 20, 3608–3616.

Mitani S (1995). Genetic regulation of mec-3 gene expression implicated in the specification of the mechanosensory neuron cell types in *Caenorhabditis elegans*. Dev Growth Diff 37, 551–557.

Moerman DG, Fire A (1997). Muscle structure, function and development. In *C. elegans II*, ed. DL Riddle, T Blumenthal, BJ Meyer, JR Priess, Plainview, NY: Cold Spring Harbor Laboratory Press, 417–470.

Moerman DG, Williams BD (2006). Sarcomere assembly in *C. elegans* muscle. In: Worm Book, ed. The *C. elegans* Research Community, WormBook, doi/10.1895/wormbook.1.81.1, www.wormbook.org.

Murton AJ, Constantin D, Greenhaff PL (2008). The involvement of the ubiquitin proteasome system in human skeletal muscle remodelling and atrophy. Biochim Biophys Acta 1782, 730–743.

Murton AJ, Greenhaff PL (2009). Muscle atrophy in immobilization and senescence in humans. Curr Opin Neurol 22, 500–505.

Petroski MD, Deshaies RJ (2005). Function and regulation of cullin-RING ubiquitin ligases. Nat Rev Mol Cell Biol 6, 9–20.

Pintard L *et al*. (2003). The BTB protein MEL-26 is a substrate-specific adaptor of the CUL-3 ubiquitin ligase. Nature 425, 311–316.

Qadota H, Benian GM (2010). Molecular structure of sarcomere-to-membrane attachment at M-lines in *C. elegans* muscle. J Biomed Biotechnol 2010, 864749.

Qadota H, Blangy A, Xiong G, Benian GM (2008a). The DH-PH region of the giant protein UNC-89 activates RHO-1 GTPase in *Caenorhabditis elegans* body wall muscle. J Mol Biol 383, 747–752.

Qadota H, McGaha LA, Mercer KB, Stark TJ, Ferrara TM, Benian GM (2008b). A novel protein phosphatase is a binding partner for the protein kinase domains of UNC-89 (obscurin) in *Caenorhabditis elegans*. Mol Biol Cell 19, 2424–2432.

Qadota H, Mercer KB, Miller RK, Kaibuchi K, Benian GM (2007). Two LIM domain proteins and UNC-96 link UNC-97/pinch to myosin thick filaments in *Caenorhabditis elegans* muscle. Mol Biol Cell 18, 4317–4326.

Roll-Mecak A, McNally FJ (2010). Microtubule-severing enzymes. Curr Opin Cell Biol 22, 96–103.

Schwechheimer C (2004). The COP9 signalosome (CSN): an evolutionary conserved proteolysis regulator in eukaryotic development. Biochim Biophys Acta 1695, 45–54.

Small TM, Gernert KM, Flaherty DB, Mercer KB, Borodovsky M, Benian GM (2004). Three new isoforms of *Caenorhabditis elegans* UNC-89 containing MLCK-like protein kinase domains. J Mol Biol 342, 91–108.

Srayko M, Buster DW, Bazirgan OA, McNally FJ, Mains PE (2000). MEI-1/MEI-2 katanin-like microtubule severing activity is required for *Caenorhabditis elegans* meiosis. Genes Dev 14, 1072–1084.

Srayko M, O'Toole ET, Hyman AA, Muller-Reichert T (2006). Katanin disrupts the microtubule lattice and increases polymer number in *C. elegans* meiosis. Curr Biol 16, 1944–1949.

Toyama Y, Forry-Schaudies S, Hoffman B, Holtzer H (1982). Efects of Taxol and Colcemid on myofibrillogenesis. Proc Natl Acad Sci USA 79, 6556–6560.

Tsutsui H, Ishihara K, Cooper G 4th (1993). Cytoskeletal role in the contractile dysfunction of hypertrophied myocardium. Science 260, 682–687.

Ventadour S, Attaix D (2006). Mechanisms of skeletal muscle atrophy. Curr Opin Rheumatol 18, 631–635.

Waterston RH (1988). Muscle. In: The Nematode *Caenorhabditis elegans*, ed. WB Wood, Plainview, NY: Cold Spring Harbor Laboratory Press, 281–335.

Waterston RH, Thomson JN, Brenner S (1980). Mutants with altered muscle structure of *Caenorhabditis elegans*. Dev Biol 77, 271–302.

Wilson KJ, Qadota H, Benian GM (2012). Immunofluorescent localization of proteins in *Caenorhabditis elegans* muscle. Methods Mol Bio 798, 171–181.

Xiong G, Qadota H, Mercer KB, McGaha LA, Oberhauser AF, Benian GM (2009). A LIM-9 (FHL)/SCPL-1 (SCP) complex interacts with the C-terminal protein kinase regions of UNC-89 (obscurin) in *C. elegans* muscle. J Mol Biol 386, 976–988.

Xu L, Wei Y, Reboul J, Vaglio Pl, Shin TH, Vidal M, Elledge SJ, Harper JW (2003). BTB proteins are substrate-specific adaptors in an SCF-like modular ubiquitin ligase containing CUL-3. Nature 425, 316–321.

Yochem J, Gu T, Han M (1998). A new marker for mosaic analysis in *Caenorhabditis elegans* indicates a fusion between hyp6 and hyp7, two major components of the hypodermis. Genetics 149, 1323–1334.

Young P, Ehler E, Gautel M (2001). Obscurin, a giant sarcomeric Rho guanine nucleotide exchange factor protein involved in sarcomere assembly. J Cell Biol 154, 123–136.